



HAL
open science

Investigations of the Photothermal Properties of a Series of Molecular Gold-bis(dithiolene) Complexes Absorbing in the NIR-III Region

Jean-Baptiste Pluta, Romain Guechaichia, Antoine Vacher, Nathalie Bellec, Sandrine Cammas-Marion, Franck Camerel

► **To cite this version:**

Jean-Baptiste Pluta, Romain Guechaichia, Antoine Vacher, Nathalie Bellec, Sandrine Cammas-Marion, et al.. Investigations of the Photothermal Properties of a Series of Molecular Gold-bis(dithiolene) Complexes Absorbing in the NIR-III Region. *Chemistry - A European Journal*, 2023, 29 (54), pp.e202301789. 10.1002/chem.202301789 . hal-04166131

HAL Id: hal-04166131

<https://hal.science/hal-04166131>

Submitted on 27 Oct 2023

HAL is a multi-disciplinary open access archive for the deposit and dissemination of scientific research documents, whether they are published or not. The documents may come from teaching and research institutions in France or abroad, or from public or private research centers.

L'archive ouverte pluridisciplinaire **HAL**, est destinée au dépôt et à la diffusion de documents scientifiques de niveau recherche, publiés ou non, émanant des établissements d'enseignement et de recherche français ou étrangers, des laboratoires publics ou privés.

Investigations of the Photothermal Properties of a Series of Molecular Gold-bis(dithiolene) Complexes Absorbing in the NIR-III Region

Jean-Baptiste Pluta,^[a] Romain Guechaichia,^[a] Antoine Vacher,^[a] Nathalie Bellec,^[a] Sandrine Cammas-Marion^[a] and Franck Camerel^{*[a]}

[a] J.-B. Pluta, R. Guechaichia, Dr. A. Vacher, Dr. N. Bellec, Dr. S. Cammas-Marion, Dr. F. Camerel
Univ. Rennes, Ecole Nationale Supérieure de Chimie de Rennes, CNRS, Institut des Sciences Chimiques de Rennes (ISCR), UMR 6226, F-35042 Rennes, France.
E-mail: franck.camerel@univ-rennes.fr
Homepage: <https://iscr.univ-rennes.fr/franck-camerel>

Supporting information for this article is given via a link at the end of the document.

Abstract: The photothermal properties of a series of neutral radical gold-bis(dithiolene) complexes absorbing in the near-infrared-III window (1550-1870 nm) have been investigated. This class of complexes was found to be good photothermal agents (PTAs) in toluene under 1600 nm laser irradiation with photothermal efficiencies around 40 and 60 % depending on the nature of the dithiolene ligand. To the best of our knowledge, these complexes are the first small molecular photothermal agents to absorb so far into the near infrared. To test their applicability in water, these hydrophobic complexes have been encapsulated into nanoparticles constituted by amphiphilic block-copolymers. Stable suspensions of polymeric nanoparticles (NPs) encapsulating the gold-bis(dithiolene) complexes have been prepared which show a diameter around 100 nm. The encapsulation rate was found to be strongly dependent on the nature of the dithiolene ligands. The photothermal properties of the aqueous suspensions containing gold-bis(dithiolene) complexes were then studied under 1600 nm laser irradiation. These studies demonstrate that water has strong photothermal activity in the NIR-III region that, cannot be overcome even with the addition of gold complexes displaying good photothermal properties.

Introduction

Photothermal therapy (PTT) is a minimally invasive, potentially selective and harmless therapeutic methodology^[1] which employs hyperthermia generated by PTAs from light energy (almost always lasers) to kill malignant cells. PTT prefers near-infrared (NIR, $\lambda = 700\text{--}1700$ nm) radiation as it offers better tissue penetration of several centimeters in biological tissues due to low light absorbance and scattering, and reduced autofluorescence of tissues and other endogenous substances. It is now accepted that the NIR window can be divided into three wavelength regions: NIR-I (700-950 nm), NIR-II (or NIR-IIa, 1000-1350 nm) and NIR-III (or NIR-IIb, 1550-1870 nm).^[2-4] However, most PTAs absorb in the NIR-I region while absorption in the NIR-II/III region ranging from 1000 to 1870 nm would allow for deeper penetration length and higher contrast in living

tissues. PTAs absorbing in the NIR-II/III region are therefore highly desirable.^[5,6]

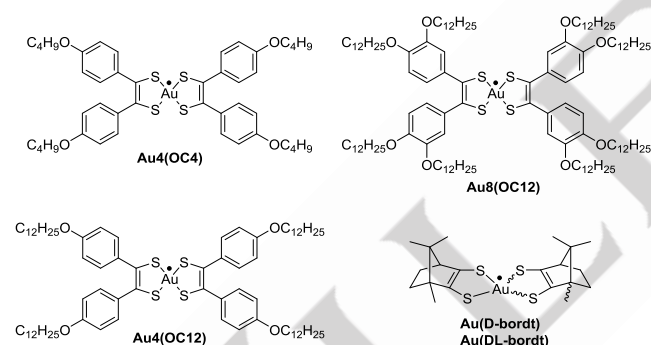
To date, several systems including Au NPs with different geometry,^[7] hybrid nanosystems,^[8,9] Fe₃O₄@CuS-PEG NPs,^[10] ammonium-tungsten-bronze nanocubes,^[11] single-walled carbon nanotubes (SWNTs),^[12,13] semiconducting quantum dots (QDs),^[14,15] rare-earth doped NPs^[16] and conjugated polymers^[17] have been explored for their photothermal activity in the NIR-II/III region. However, considering the translation of NIR-II/III PTAs into clinical applications, small-molecules remain the most desirable and optimal candidates because of their high biocompatibility, fast excretion, quality control under the current Good Manufacturing Practice (cGMP) conditions, and easy and robust preparation. Therefore, developing small molecule based NIR-II/III PTAs with desirable chemical and physical properties, favorable excretion pharmacokinetics, minimal cellular toxicity and clinical translation ability is crucial and highly demanded. Molecular cyanine dyes and conjugated small molecules (CSMs) are popular small-molecule NIR-II/III PTAs.^[18-20] However, their isolation requires intensive synthetic work and their absorption maxima barely exceed 1100 nm. Although the excellent photophysical and photochemical performance exhibited by these fluorophores justifies their application in biological imaging and tumor therapy, new NIR-II/III PTAs with a stable structure capable of absorbing between 1000 and 1870 nm and more facile synthetic routes are needed.

Because of their small Highest Occupied Molecular Orbital-Lowest Unoccupied Molecular Orbital (HOMO-LUMO) gap (< 1.5 eV), neutral nickel-bis(dithiolene) complexes strongly absorb in the NIR 800-1100 nm region, with ϵ values up to 40,000 M⁻¹.cm⁻¹. Such complexes are highly stable under laser irradiation and are able to convert light into heat with high efficiencies reaching up to 40-50%. These photothermal effects have been particularly investigated by our group for applications in soft matter (liquid crystals, gels, and NPs).^[21] For example, hydrophobic Ni dithiolene complexes were designed for their encapsulation in block copolymeric NPs for PTT under laser irradiation.^[22] However, these studies were limited to the NIR-I window by the 800-1000 nm absorption of neutral Ni-bis(dithiolene) complexes.

Addressing the NIR-II/III window ranging from 1000 to 1870 nm would allow for a better tissue penetration depth and a higher maximum permissible exposure value. It is possible to approach the NIR-II range by introducing strong electron donating groups on Ni-bis(dithiolene) complexes but the obtained complexes are highly susceptible to oxidation, decreasing their stability and applicability.^[23]

Recently, neutral radical Au complexes displaying a strong absorption band at lower energy between the HOMO and the SOMO (Singly Occupied Molecular Orbital), in the 1200-1600 nm range have been reported.^[24,25] Thus, efficient NIR-III PTAs can in principle be obtained if gold is used instead of nickel, with the possible extra advantage of decreased toxicity compare to nickel complexes. However, their photothermal activity under laser irradiation have not been yet evaluated.

The objective of this work is therefore to demonstrate that Au-bis(dithiolene) complexes are effective PTAs in the NIR-III window and to evaluate their potential for PTT in aqueous biological medium. For this purpose, several hydrophobic Au-bis(dithiolene) with various substitution patterns were synthesized (Scheme 1). Their photothermal properties were first investigated in toluene solutions and compared to those of the parent Ni-bis(dithiolene). For envisioned PTT applications, the hydrophobic gold complexes were finally encapsulated into biocompatible and biodegradable NPs based on poly(benzyl malate), PMLABe, derivatives and their photothermal properties were then evaluated in water.



Scheme 1. Overview of the five Au-bis(dithiolene) complexes investigated in this work.

Results and Discussion

The five gold-bis(dithiolene) complexes have been synthesized following procedures reported in the literature (see Supporting Information for full details).^[25,26] These different complexes were selected to study the impact of the dithiolene core and the carbon chain number on the photothermal properties and the encapsulation rate. The two complexes with aryl groups **Au4(OC4)** and **Au4(OC12)** were synthesized following the same method, starting from commercially available *para*-anisil (Scheme S1). The phenolic groups of *para*-anisil are deprotected under acidic conditions and then react with bromoalkane in a Williamson reaction. The diketone is sulfured

with phosphorus pentasulfide in 1,3-Dimethyl-2-imidazolidinone (DMI). The intermediate is not isolated and immediately reacted with the gold salt to afford a precipitate. After reaction, the mixture is poured into a large amount of ethanol to afford the neutral gold complex as a precipitate, which is finally recrystallized by slow evaporation of dichloromethane (DCM) in a DCM/methanol mixture. The synthetic route to obtain **Au8(OC12)** is similar to the one described previously, but starting from veratraldehyde (Scheme S2). Veratraldehyde is homocoupled through a benzoin condensation in the presence of KCN. The resulting benzoin is oxidized with copper sulfate to form the diketone. The synthetic pathway is then identical to the one described for **Au4(OC4)** and **Au4(OC12)**. Finally, **Au(D/DL-bordt)** complexes are synthesized in one step from commercially available D/DL-camphorquinone, using the same protocol with phosphorus pentasulfide in DMI as for the other complexes (Scheme S3). The purity of all the gold complexes was ascertained by ¹H and ¹³C NMR, Maldi-tof and elemental analysis. The radical character of the complexes was confirmed by The X-band EPR measurements (Figure S1). The neutral gold complexes dissolved in CH₂Cl₂ solution display at room temperature one single Lorentzian line at $g = 2.011$. In frozen solution, anisotropic signals around $g \approx 2$ typical of an $S = \frac{1}{2}$ system with rhombic g factors are observed (Table S1). The g tensor principal values collected in Table S1 compare well with the values already reported for gold bis(dithiolene) complexes.^[24,25,26]

The absorption properties of the five hydrophobic gold complexes have been studied in toluene. All the complexes display a strong absorption peak in the NIR window (Figure 1). **Au4(OC4)** and **Au4(OC12)** show an absorption maximum at 1568 nm with strong molar extinction coefficients of 25,535 and 27,395 M⁻¹.cm⁻¹, respectively. This low-energy absorption band is characteristic of neutral radical gold-bis(dithiolene) complexes and is attributed to an electronic transition from the HOMO to the SOMO.^[24,25] The position of this low energy absorption band does not vary with the length of the carbon chains and the extinction coefficients are only weakly affected (around 7% variation). **Au4(OC4)** and **Au4(OC12)** also display a strong absorption band centered at 358 nm (Figure 1) in the UV region assigned to $\pi-\pi^*$ transitions localized on the dithiolene ligands. Introduction of four additional dodecyloxy carbon chains on **Au8(OC12)** leads to a bathochromic shift of the absorption band by 46 nm at 1614 nm and the extinction coefficient is strongly reduced to 17,438 M⁻¹.cm⁻¹. **Au(D-bordt)** and **Au(DL-bordt)** also display a strong absorption band in the NIR-III region of similar shape with a maximum at 1500 nm. This band is hypsochromically shifted compared to the other dithiolene complexes obtained from benzil derivatives. The molar extinction coefficients of 17,191 M⁻¹.cm⁻¹ for **Au(D-bordt)** and of 17,589 M⁻¹.cm⁻¹ for **Au(DL-bordt)** are comparable with that measured for **Au8(OC12)**. No real difference on the absorption properties has been observed between the enantiopure **Au(D-bordt)** complex and the racemic ligand mixture of **Au(DL-bordt)**, meaning that the optical properties are not sensitive to the chirality of the dithiolene ligand.

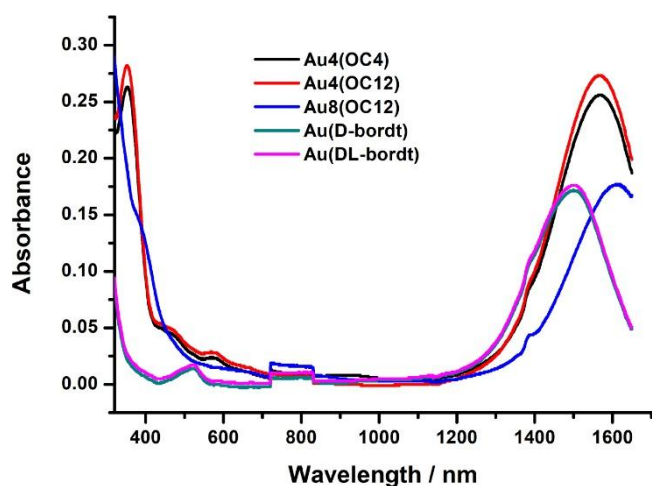


Figure 1. UV-vis-NIR absorption profiles of the five studied complexes. $\lambda = 1650\text{--}320$ nm; reference = toluene; $C = 10^{-5}$ M; detection limit = 1650 nm in toluene with a quartz cuvette.

The length of alkoxy chains weakly affect the absorption properties of the gold-dithiolene complexes but are more drastically affected by their number and the nature of the dithiolene ligand. The chirality of the ligands also seems to have little to no influence on the absorption properties in solution. The exceptional absorption properties of Au-bis(dithiolene) complexes in the NIR-III region around 1600 nm therefore

prompted us to explore their photothermal properties under laser irradiation.

The photothermal properties of the five gold complexes were investigated in toluene in order to limit evaporation ($b_p = 110.6$ °C) since high temperatures can be reached during laser irradiation. The five complex solutions at $C = 10^{-5}$ M were irradiated with a 1600 nm continuous diode laser with a power of $3 \text{ W}\cdot\text{cm}^{-2}$ (Figure 2, S5-S8). In order to extract the photothermal efficiency η , thermal equilibrium must be reached (the maximum attained temperature T_{max} is constant). For the five gold complex solutions, thermal equilibrium is reached in 18 min. The combined results with confidence intervals are shown in Table 1. High maximum temperatures ranging from 67 °C to 82 °C have been measured under laser irradiation. It should be noticed that in the absence of complex, a limited temperature increase of only 13.1 °C was observed after 18 min of irradiation under $3 \text{ W}\cdot\text{cm}^{-2}$ laser irradiation in pure toluene, confirming the strong photothermal activity of the gold-bis(dithiolene) complexes at 1600 nm. The temperature elevation is higher for **Au4(OC4)** and **Au4(OC12)** than for **Au8(OC12)**, **Au(D-bordt)** and **Au(DL-bordt)**. This discrepancy is attributed in part (*vide infra*) to the absorption differences observed on the UV curves at 1600 nm (Figure 1). These complexes were found to be highly photothermally stable. No fatigue was observed after several heating and cooling cycles (Figure S9-S13).

Table 1. Values with confidence interval ($N = 6$) for ϵ_{laser} in toluene; T_{max} and η at 10^{-5} M and $3 \text{ W}\cdot\text{cm}^{-2}$, at 1600 nm in toluene, for the five studied complexes (Student interval, $\alpha = 5\%$)

Complex	$\epsilon_{\text{laser}} (\text{M}^{-1}\cdot\text{cm}^{-1})$	$T_{\text{max}} (\text{°C})$	$\Delta T (\text{°C})$	$\eta (\%)$
Au4(OC4)	$24,335 \pm 690$	79.8 ± 3.1	55.3 ± 1.0	39.3 ± 3.9
Au4(OC12)	$26,055 \pm 162$	82.4 ± 3.5	57.3 ± 1.1	40.2 ± 3.9
Au8(OC12)	$17,372 \pm 478$	69.8 ± 3.2	44.6 ± 1.3	41.1 ± 3.8
Au(D-bordt)	$9,262 \pm 246$	67.5 ± 0.9	40.0 ± 0.4	66.4 ± 1.2
Au(DL-bordt)	$9,477 \pm 137$	67.6 ± 0.4	40.9 ± 0.6	63.4 ± 2.3

The photothermal yield (or conversion efficiency) η was evaluated by monitoring the temperature profile for 18 min under continuous laser irradiation at 1600 nm and for 18 min after turning off the laser (Figure 2). The η values were calculated according to the formula (1) reported by Roper *et al.*:^[29]

$$\eta (\%) = 100 \frac{hS(T_{\text{max}}^{\text{PTA}} - T_{\text{amb}}) - Q^{\text{ref}}}{P(1 - 10^{-A})} \quad (1)$$

Formula 1. Empirical expression of the photothermal yield.

The time constant for heat transfer $\tau_s = (m \cdot c_p) / (hS)$ is determined by applying the linear time from the cooling period (from 1080 to 2160 s) versus negative natural logarithm of the driving force temperature (Figure 2 insert).

The photothermal yields of **Au(D-bordt)** and **Au(DL-bordt)** are about 65%, much higher than the benzil derivatives, which are about 40%, indicating that the bordt ligand favors deactivation through non-radiative pathways more than the benzil derivatives with their long carbon chains. The measured photothermal yields of around 40% for the benzil derivatives compare well with those measured on the parent nickel-bis(dithiolene) complexes^[30]. It seems that the photothermal yield depends strongly on the

nature of the dithiolene ligand more so than the nature of the metal center or the wavelength of the laser.

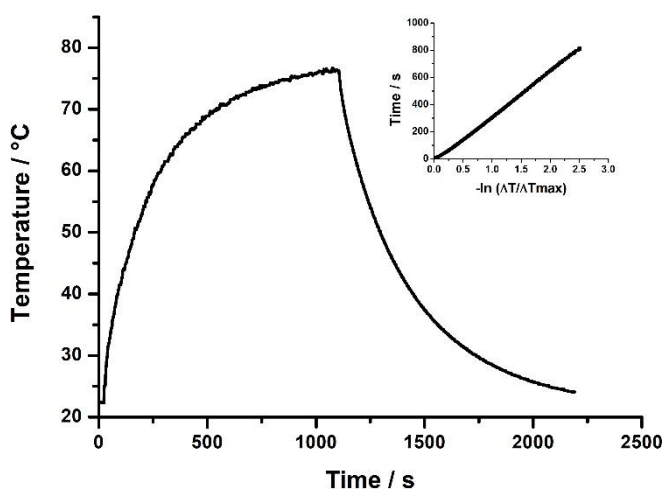


Figure 2. Representative temperature profile recorded on **Au4(OC4)** in toluene solution at 1.0×10^{-5} M when illuminated with a 1600 nm laser ($3 \text{ W}\cdot\text{cm}^{-2}$) for 18 min and after turning off of the laser for 18 min. (insert : Linear time from the cooling period (from 1080 to 2160 s) versus negative natural logarithm of the driving force temperature).

As can be seen, the temperature increase ΔT depends on the photothermal yield of the compound but also on its molar extinction coefficient at the irradiation wavelength. Indeed, a compound can strongly absorb the laser but if the photothermal efficiency is low, the temperature increase will be low. In the same manner, if the compound has a good photothermal efficiency but a low absorption at the irradiation wavelength, the temperature increase will also be limited. The temperature increase with a compound that strongly absorbs the laser and has a good photothermal efficiency will be much higher than that

with a compound that has a low absorption and a low ability to convert light into heat. Thus, to be considered as a good PTA, the compound should strongly absorb at the irradiation wavelength and should also display a high photothermal yield. For these reasons, in order to better rank the molecular PTAs, a new photothermal index (I_{PT}) strongly resembling the brilliance in fluorescence, which accounts for both the absorption coefficient and the photothermal yield, was recently introduced.^[31]

Table 2. Values with confidence interval (N= 6) for I_{PT} in toluene at 1600 nm, for the five studied complexes.

Complex	Au4(OC4)	Au4(OC12)	Au8(OC12)	Au(D-bordt)	Au(DL-bordt)
$I_{PT}(1600)$	9.6 ± 1.0	10.5 ± 1.0	7.1 ± 0.7	6.1 ± 0.2	6.0 ± 0.2

$$I_{PT}(\lambda) = 10^{-5} \varepsilon_{\lambda} \eta \quad (2)$$

Formula 2. Definition of the photothermal index I_{PT} for a set wavelength λ .

This photothermal index allows for a proper ranking of PTAs irradiated at the same wavelength. The only limitation of this photothermal index is that all the PTAs have to be studied in the same solvent, since the molar absorption coefficient depends on the nature of the solvent.

Based on this formula, the I_{PT} at 1600 nm of each compound has been calculated using the molar absorption coefficient calculated at 1600 nm (ε_{1600}) and are reported in Table 2.

The best molecular PTA at 1600 nm is therefore **Au4(OC12)**, closely followed by **Au4(OC4)**. Despite, their good photothermal efficiencies, the **Au(D-bordt)** and the **Au(DL-bordt)** are less efficient photothermal agents due to their low molar absorption coefficients at 1600 nm. All these complexes are less efficient PTAs than their nickel counterparts absorbing at 940 nm with $I_{PT}(940)$ around 18 but to the best of our knowledge, these gold complexes are the first molecular PTAs in the NIR-III region.

Table 3 gathers all the molecular PTAs with an absorption maximum in the NIR-II/III region above 1000 nm. Their full chemical structure is given in Supporting Information (Scheme S4). As can be seen, there are only a few candidate molecules, and despite a good photothermal efficiency, their maximum absorption barely exceeds 1100 nm.^[32–39] Their photothermal indexes cannot be calculated for comparison because all these compounds were encapsulated for measurements (no accurate molar extinction coefficients) and solvents other than toluene were used. In the field of organic molecular NIR-III components, some expanded porphyrinoids were synthesized by Wang *et al.* as absorbing and emitting dyes.^[40] Their emissive and photoacoustic properties were explored, but not their potential photothermal effect. In that sense, gold-bis(dithiolene) complexes are exceptional since they are easily synthesized and display a good photothermal activity far in the NIR region.

Table 3. Reported NIR-II/III molecular PTAs having an absorption maxima above 1000 nm. Molecular structures are presented in Supporting Information (Scheme S4). The λ_{max} and η values were obtained only with encapsulated PTAs.

Name	λ_{max} (nm)	η (%)	ref
BAF ₄	1000	80	32
NiBD-Cz	1010	63.6	33
IDI	1100	75.2	34
IR-SS	1060	77	35
CPDT-T	1054	49	36
IR1048-COOH	1039	44.1	37
LET-1052	1052	57.2	38
Zn ₄ -H ₂ [Pc(OC ₁₂ H ₁₇) ₂₄]	1040	75.2	39

All of these gold-dithiolene complexes are good PTAs for the potential application in photothermal therapy in the NIR-III region. However, to be useful, the photothermal activity of these complexes should overcome the possible photothermal activity of water which strongly absorb in the NIR-III region. It should be noted that to our knowledge, the photothermal activity of water under laser irradiation in the NIR-III region has not yet been studied.

To overcome the problems linked to hydrophobicity of the gold complexes for applications in water, we have encapsulated the gold complexes into the inner-core of biocompatible and biodegradable NPs constituted by the amphiphilic block copolymers PEG₄₂-*b*-PMLABE₇₃ (See supporting information for synthetic details and characterizations).^[41] NPs encapsulating the gold complexes were prepared using the nanoprecipitation method described by Thioune *et al.* based on the self-assembly of hydrophobic or amphiphilic (co)polymer in aqueous medium.^[42] For the nanoprecipitation, optimized parameters such as the initial polymer concentration, the addition rate, the organic solvent/water ratio and the stirring speed have been used.^[43]

Briefly, a solution of complex and polymer in THF was added to a strongly stirred volume of water. The resulting suspension is concentrated under reduced pressure and filtered under ultracentrifugation over Micro-Con filters. The retentate was harvested and dispersed in ultrapure water in order to get suspensions of 10 mg.mL⁻¹ of polymer and, theoretically, 1 mg/mL of complex. A batch of empty NPs was also prepared.

The NPs' hydrodynamic diameter D_h and dispersity PDI were measured by Dynamic Light Scattering (DLS) right after preparation, at d+1 and d+7 (Figure 3a and 3b; Figure S14-S18). The encapsulation efficiency (EE) was calculated by using the Beer-Lambert law on a known amount of freeze-dried NPs encapsulating the gold complexes redissolved in THF (Table S2). The samples were freeze-dried to remove adsorbed water. The transmission electron microscopy (TEM) images recorded on the empty PEG₄₂-*b*-PMLABe₇₃ NPs confirm a spherical shape with an average diameter of 53±1 nm (Figure 4). The average diameter measured by TEM is lower than the one measured by DLS because the hydration layer is not visible by TEM. Strong differences in hydrodynamic diameter (D_h) can be observed between the empty nanoparticles and the particles encapsulating the gold complexes (Figure 3a). The D_h of the empty NPs is around 125 nm and the encapsulation of the gold complexes into PEG₄₂-*b*-PMLABe₇₃ based nanoparticles led to a significant decrease of the D_h values. The D_h appears to strongly decrease with the increase of the length and the number of carbon chains. The decrease of D_h can likely be attributed to stronger hydrophobic interactions between the polymer and the complex going from the **Au4(OC4)** to **Au8(OC12)**. The encapsulation of **Au(D-bordt)** complex, without phenyl rings, led to an increase of the D_h value, probably because this complex does not allow π -stacking interactions with the lateral chains of the polymer. The PDI values, ranging from 0.18 to 0.29, highlighted that the prepared nanoparticles suspensions were monodisperse (Figure 3b). These formulations were found to be stable for at least one month when stored at 4°C (Figure S19).

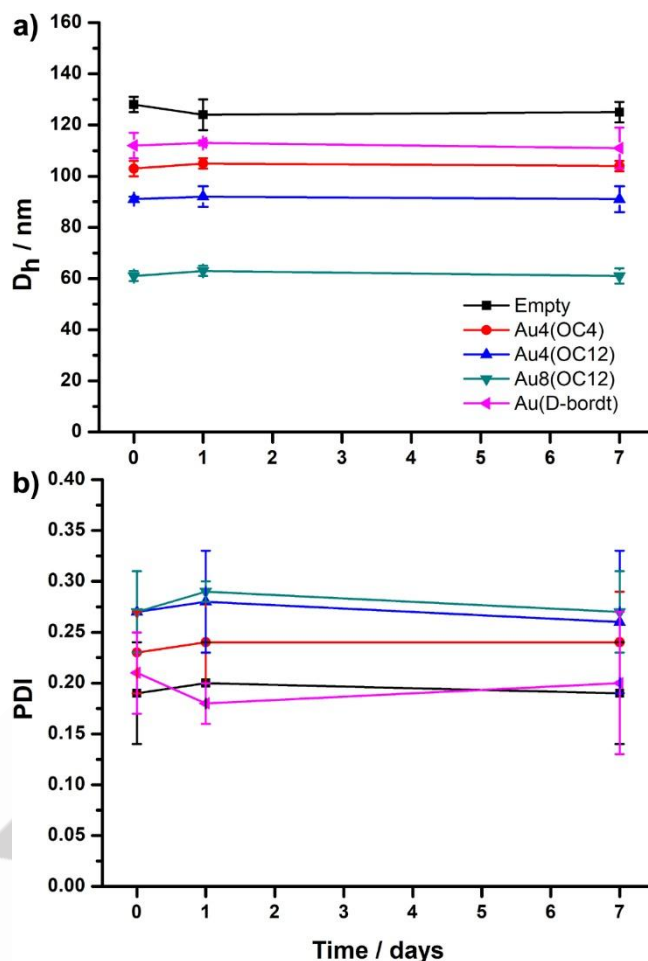


Figure 3. Evolution of D_h (a) and PDI (b) of NPs, values with confidence interval (N= 3).

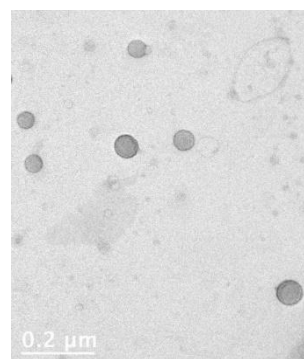


Figure 4. Image obtained by TEM of the PEG₄₂-*b*-PMLABe₇₃ NPs using a Jeol 2010 LaB6 apparatus operating under a voltage of 80KeV. The sample was previously stained with 0.1v% of phosphotungstic acid.

Determination of the encapsulation efficiency (EE) (see Supporting Information) shows that the two complexes **Au4(OC12)** (68 %) and **Au4(OC4)** (47 %) with four long carbon chains are much more efficiently encapsulated than the complex **Au8(OC12)** (6 %) with eight carbon chains or than the **Au(D-bordt)** complex (8 %). With four alkoxy chains, the longer the chain, the better the encapsulation efficiency is, probably by giving the complex a more hydrophobic nature. For **Au8(OC12)** and **Au(D-bordt)**, a more hydrophobic character and higher steric constraints probably prevent the encapsulation of the complexes, especially in the PEG outer shell.

Based on the photophysical measurements performed in toluene and the encapsulation rate measured, we focused our photothermal investigations in water on the aqueous NPs suspension of PEG₄₂-*b*-PMLABe₇₃ polymer encapsulating **Au4(OC12)** complex ($C_{\text{pol}} = 500 \mu\text{g.mL}^{-1}$, $C_{\text{complex}} = 34 \mu\text{g.L}^{-1}$). The photothermal properties of the suspension of PEG₄₂-*b*-PMLABe₇₃ NPs incorporating **Au4(OC12)** complex in the NIR-III region were evaluated by irradiating a dilute aqueous suspensions with a continuous 1600 nm laser at 2 W.cm^{-2} . The solution was irradiated for 10 min (600 s). After turning off the laser, the cooling regime of the solutions was recorded for another 10 min. Figure 5 shows a typical recorded temperature increase profile. For comparison, pure water and an aqueous PEG₄₂-*b*-PMLABe₇₃-based NPs suspension without gold complex was measured under the same conditions.

As can be clearly seen, the temperature increase under 1600 nm laser irradiation is comparable in pure water and in the suspension of PEG₄₂-*b*-PMLABe₇₃ NPs incorporating **Au4(OC12)**, meaning that the photothermal effect observed is mainly due to the water. This result also indicates that water strongly absorb the 1600 nm laser irradiation. To confirm this, UV-vis-NIR absorption profiles of water diluted in THF at various proportions have been recorded (Figure 6). Indeed, water strongly absorbs NIR light from 1300 nm to 1650 nm with a maximum at 1460 nm. The UV-vis-NIR absorption spectra of water in THF is in accordance with the near infrared spectra of pure water reported in the literature showing a clear absorption band in the 1300-1650 nm range.^[44,45] This strong absorption is at the origin of the photothermal effect detected under 1600 nm laser irradiation. The photothermal properties of the gold complexes are therefore masked by those of the water. With a lower-power laser (0.75 W.cm^{-2}), the temperature increase in pure water remains significant and the photothermal properties of the gold complexes are still masked (Figure 7). These measurements also lead to the conclusion that laser irradiation between 1300 nm and 1650 nm cannot be used for deep and localized *in vivo* photothermal therapy. PTAs absorbing beyond 1300 nm will also be useless for *in vivo* applications, since they will absorb less than water at the concentration generally used (few $\mu\text{g.mL}^{-1}$). This raises the question of the relevance of developing new PTAs absorbing in the NIR-III window between 1300 and 1870 nm.

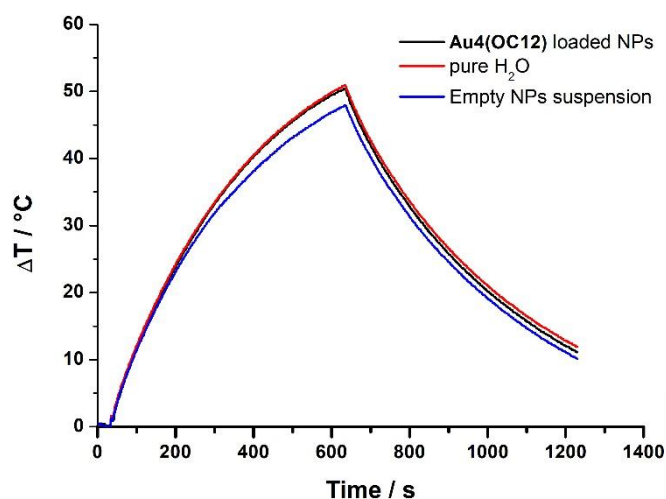


Figure 5. Temperature increase recorded on a NPs suspension of PEG₄₂-*b*-PMLABe₇₃ polymer in water, a NPs suspension of PEG₄₂-*b*-PMLABe₇₃ polymer encapsulating **Au4(OC12)** complex in water ($C_{\text{pol}} = 500 \mu\text{g.mL}^{-1}$) and on pure water under 1600 nm laser irradiation (10 min irradiation 2 W.cm^{-2} + 10 min laser OFF).

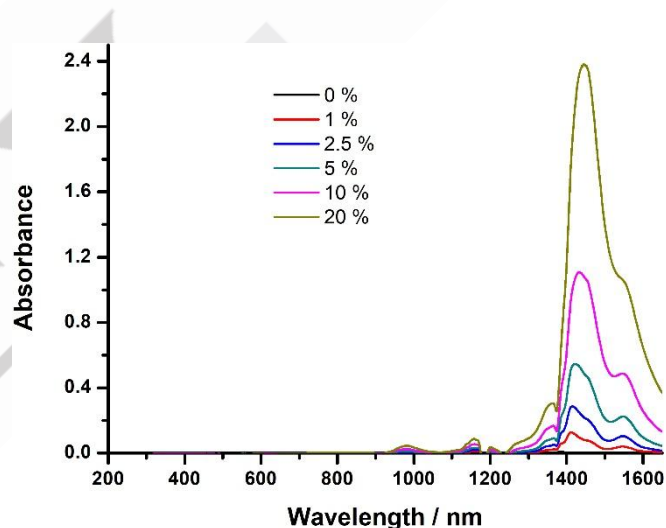


Figure 6. UV to NIR absorption profile of water in THF in %v/v (detection limit= 1650 nm in toluene with a quartz cuvette).

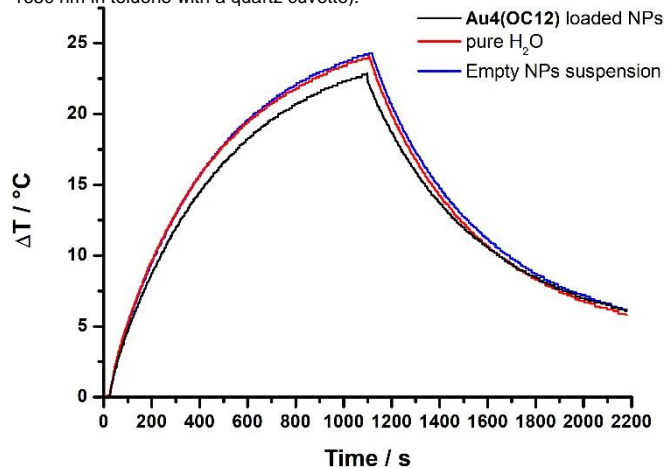


Figure 7. Temperature increase recorded on a NPs suspension of PEG₄₂-*b*-PMLABe₇₃ polymer in water, a NPs suspension of PEG₄₂-*b*-PMLABe₇₃ polymer encapsulating **Au₄(OC₁₂)** complex in water ($C_{\text{pol}} = 500 \mu\text{g.mL}^{-1}$) and

on pure water under 1600 nm laser irradiation (18 min irradiation 0.75 W.cm⁻² + 18 min laser OFF).

The photothermal activity of water under irradiation at 1600 nm was confirmed by measuring the temperature rise of pure water with different laser powers (Figure 8). In contrast to what was measured on pure toluene ($\Delta T = 13.1$ °C for 18 min with 3 W.cm⁻²), a much larger temperature increase ($\Delta T = 75$ °C, sufficient to reach boiling point in <10 min), was measured under 3 W.cm⁻² laser irradiation. As shown in the figure, the temperature rise also increases with the power of the laser.

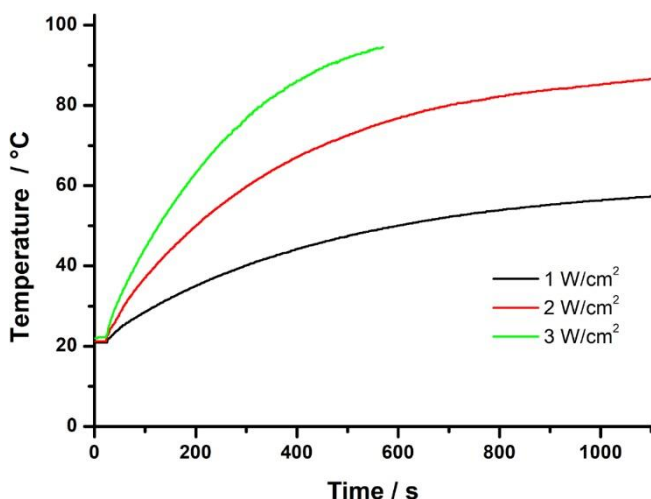


Figure 8. Irradiation of pure water at 1600 nm. The measurement was stopped when the temperature reached 95°C before 18 min.

Conclusion

The photothermal activity of a series of four gold-bis(dithiolene) complexes absorbing in the NIR-III region have been evaluated under 1600 nm laser irradiation. In toluene solution, these complexes display a good photothermal activity with photothermal efficiencies around 40 and 60% depending on the nature of the dithiolene ligand. The photothermal index at 1600 nm with a good confidence interval was calculated in order to rank these complexes as a function of their photothermal efficiency. **Au4(OC12)** is the best molecular PTA at 1600 nm, followed closely by the **Au4(OC4)** complex. **Au(D-bordt)** and the **Au(DL-bordt)** are less efficient PTAs due to their low molar absorption coefficient at 1600 nm. For evaluation in water, these hydrophobic complexes have been then encapsulated into nanoparticles constituted by an amphiphilic block copolymers PEG₄₂-*b*-PMLABe₇₃. NPs with low polydispersity were isolated but determination of the encapsulation efficiency showed that the two complexes **Au4(OC12)** and **Au4(OC4)** with four long carbon chains are much more efficiently encapsulated. Investigation of the photothermal properties of these NPs encapsulating gold-bis(dithiolene) photothermal agent in water under 1600 nm laser irradiation revealed that the photothermal activity of the gold complexes is completely masked by the strong photothermal activity of water. The results obtained in water clearly show that these photothermal compounds absorbing between 1300 and 1650 nm will be useless for PTT or

photothermal catalysis in water, since water is a good photothermal medium by itself. Although NIR-III appears to be a target for imaging, it is unusable for PTT and efforts should instead be focused on NIR-II compounds absorbing between 1000 and 1300 nm. Nevertheless, these long-wavelength molecular photothermal absorbers can be of great interest to develop new NIR sensors and detectors as well as photo-responsive materials for applications in energy conversion or in soft-robotics. Recently, a new approach based on ligand scrambling of gold-bis(dithiolene) complexes in order to tune the absorption maximum has been reported^[26] and could be used to develop dithiolene complexes absorbing at more appropriate wavelengths below 1300 nm for applications in biological medium. Works along these lines are currently being developed in our laboratory.

Experimental part

All the chemicals and solvents used for synthesis and physical characterizations were of reagent grade. Chromatography purifications were done by hand on silica gel (40-60 μm) Acros; or on a Combiflash Rf with Redistep silica columns (4-400 g, 35-70 μm). NMR experiments were done on a spectrometer Bruker AV III 300 MHz. Maldi-tof experiments were done on a spectrometer Bruker Microflex LT, using dithranol (dith) or DCTB for the matrix. Spectrophotometry experiments were done on a spectrometer Shimadzu UV3600 Plus, in quartz cuvettes, and the molar attenuation coefficient ϵ was calculated according to the Beer-Lambert law. The photothermal studies were done using a 1600 nm laser (Changchun New Industries Optoelectronics, Model FC-W-1600-10W-BI90071) in a glass cuvette with a thermocouple PerfectPrime (model TC0520) device, run and saved on computer with the dedicated software SE520. Confidence intervals were calculated with samples of size N (given each time) and Student's coefficient ($\alpha = 5\%$). Size exclusion chromatography (SEC) measurements were performed in tetrahydrofuran (THF) at 40°C (flow rate= 1.0 mL/min) on a GPC2502 Viscotek apparatus equipped with a refractive index detector Viscotek VE 3580 RI, a guard column Viscotek TGuard, Org 10 x 4.6 mm, a LT5000L gel column (for samples soluble in organic medium) 300 x 7.8 mm and a GPC/SEC OmniSEC software. EPR spectra were obtained on a X-band Bruker EMX 8/2.7 spectrometer equipped with liquid nitrogen cooling system. Simulations were performed with Bruker WinEPR Symphonia. Infrared absorption spectra were studied within the mid-IR range (600 - 4000 cm⁻¹) by using JASCO 4600 FT-IR spectrometer equipped with a PIKE ATR diamond apparatus. TEM analyses of the NPs were realized at the "Institute des Sciences Chimiques de Rennes". Each sample (5 μL) was deposited on a Formvar-carbon film coated on a copper grid (300 mesh). After 6 min, the excess of water was removed by absorption with filter paper and the sample was stained with phosphotungstic acid (0.1 v%) for 30 s. The grid was then placed under the electron beam. The microscope used was a JEOL 2010 LaB6 operating at 80 kV. The camera, on which the images were recorded, was a GATAN Orius 200D

CCD (Charge Coupled Device) camera. All the gold-bis(dithiolene) complexes have been synthesized following procedures reported in the literature (see Supporting Information for full synthetic details).^[25,26] PEG₄₂-*b*-PMLABe₇₃ block copolymers were synthesized as previously described^[27]. Briefly, the benzyl malolactonate, monomer obtained in four steps starting from aspartic acid^[28], was polymerized by anionic ring-opening polymerization in presence of the tetraethylammonium salt of α -methoxy- ω -carboxylate PEG₄₂ as initiator. After purification, the block copolymers were characterized by proton NMR (structure and molar mass of the PEG-PMLABe polymer) and size exclusion chromatography in THF (see supporting information).

Supporting Information

Materials and methods. Full synthetic details and characterizations of the proligands and of the gold complexes. Synthesis of the block-copolymer PEG₄₂-*b*-PMLABe₇₃ with ¹H NMR and SEC characterizations. Description of the nanoprecipitation methods and determination of the encapsulation efficiency. Temperature profiles recorded for all the complexes in toluene solution under laser irradiation at 1600 nm laser (3 W.cm⁻²). Stability measurements of the complexes in toluene solution after five consecutive heating/cooling cycles under 1600 nm laser irradiation (3 W.cm⁻²). Results of the dynamic light scattering (DLS) measurements. Study of the stability of nanoparticles when stored at 4°C. List of the NIR-II/III molecular PTAs reported in the literature.

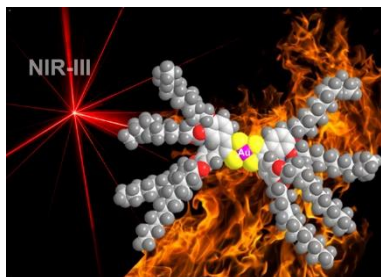
Acknowledgements

N.B., S.C.-M. and F.C. acknowledge the CNRS, the University of Rennes and the "Ligue contre le cancer CD 35, 45, 85" for their financial support. This work was also partly funded by France Life Imaging (grant ANR-11-INBS-0006).

Keywords: Gold-bis(dithiolene) complexes • Photothermal index • Nanoparticles • Molecular photothermal agent • NIR-III Laser irradiation

- [1] D. Zhi, T. Yang, J. O'Hagan, S. Zhang, R. F. Donnelly, *J. Controlled Release* **2020**, 325, 52–71.
- [2] E. Hemmer, N. Venkatachalam, H. Hyodo, A. Hattori, Y. Ebina, H. Kishimoto, K. Soga, *Nanoscale* **2013**, 5, 11339.
- [3] A. M. Smith, M. C. Mancini, S. Nie, *Nat. Nanotechnol.* **2009**, 4, 710–711.
- [4] L. Sordillo, S. Pratavieira, Y. Pu, K. Salas-Ramirez, L. Shi, L. Zhang, Y. Budansky, *Proc. SPIE - Int. Soc. Opt. Eng.* **2014**, 8940, DOI 10.1117/12.2040604.
- [5] E. Hemmer, A. Benayas, F. Légaré, F. Vetrone, *Nanoscale Horiz.* **2016**, 1, 168–184.
- [6] S. Chinnathambi, N. Shirahata, *Sci. Technol. Adv. Mater.* **2019**, 20, 337–355.
- [7] P. Vijayaraghavan, C.-H. Liu, R. Vankayala, C.-S. Chiang, K. C. Hwang, *Adv. Mater.* **2014**, 26, 6689–6695.
- [8] M.-F. Tsai, S.-H. G. Chang, F.-Y. Cheng, V. Shanmugam, Y.-S. Cheng, C.-H. Su, C.-S. Yeh, *ACS Nano* **2013**, 7, 5330–5342.
- [9] X. Ding, C. H. Liow, M. Zhang, R. Huang, C. Li, H. Shen, M. Liu, Y. Zou, N. Gao, Z. Zhang, Y. Li, Q. Wang, S. Li, J. Jiang, *J. Am. Chem. Soc.* **2014**, 136, 15684–15693.
- [10] Z.-C. Wu, W.-P. Li, C.-H. Luo, C.-H. Su, C.-S. Yeh, *Adv. Funct. Mater.* **2015**, 25, 6527–6537.
- [11] C. Guo, H. Yu, B. Feng, W. Gao, M. Yan, Z. Zhang, Y. Li, S. Liu, *Biomaterials* **2015**, 52, 407–416.
- [12] G. Hong, S. Diao, J. Chang, A. L. Antaris, C. Chen, B. Zhang, S. Zhao, D. N. Atochin, P. L. Huang, K. I. Andreasson, C. J. Kuo, H. Dai, *Nat. Photonics* **2014**, 8, 723–730.
- [13] J. T. Robinson, G. Hong, Y. Liang, B. Zhang, O. K. Yaghi, H. Dai, *J. Am. Chem. Soc.* **2012**, 134, 10664–10669.
- [14] Y. Zhang, G. Hong, Y. Zhang, G. Chen, F. Li, H. Dai, Q. Wang, *ACS Nano* **2012**, 6, 3695–3702.
- [15] G. Chen, F. Tian, Y. Zhang, Y. Zhang, C. Li, Q. Wang, *Adv. Funct. Mater.* **2014**, 24, 2481–2488.
- [16] D. J. Naczynski, M. C. Tan, M. Zevon, B. Wall, J. Kohl, A. Kulesa, S. Chen, C. M. Roth, R. E. Riman, P. V. Moghe, *Nat. Commun.* **2013**, 4, 2199.
- [17] G. Hong, Y. Zou, A. L. Antaris, S. Diao, D. Wu, K. Cheng, X. Zhang, C. Chen, B. Liu, Y. He, J. Z. Wu, J. Yuan, B. Zhang, Z. Tao, C. Fukunaga, H. Dai, *Nat. Commun.* **2014**, 5, 4206.
- [18] Q. Chen, J. Chen, M. He, Y. Bai, H. Yan, N. Zeng, F. Liu, S. Wen, L. Song, Z. Sheng, C. Liu, C. Fang, *Biomater. Sci.* **2019**, 7, 3165–3177.
- [19] W. Shao, Q. Wei, S. Wang, F. Li, J. Wu, J. Ren, F. Cao, H. Liao, J. Gao, M. Zhou, D. Ling, *Mater. Horiz.* **2020**, 7, 1379–1386.
- [20] H. Dai, Q. Shen, J. Shao, W. Wang, F. Gao, X. Dong, *The Innovation* **2021**, 2, 100082.
- [21] F. Camerel, M. Fourmigué, *Eur. J. Inorg. Chem.* **2020**, 2020, 508–522.
- [22] M. Ciancone, K. Mebrouk, N. Bellec, C. L. Goff-Gaillard, Y. Arlot-Bonnemains, T. Benvegna, M. Fourmigué, F. Camerel, S. Cammas-Marion, *J. Mater. Chem. B* **2018**, 6, 1744–1753.
- [23] U. T. Mueller-westerhoff, D. I. Yoon, K. Plourde, *Mol. Cryst. Liq. Cryst. Inc. Nonlinear Opt.* **1990**, 183, 291–302.
- [24] R. Perochon, L. Piekara-Sady, W. Jurga, R. Clérac, M. Fourmigué, *Dalton Trans.* **2009**, 0, 3052–3061.
- [25] R. Perochon, P. Davidson, S. Rouzière, F. Camerel, L. Piekara-Sady, T. Guizouarn, M. Fourmigué, *J. Mater. Chem.* **2011**, 21, 1416–1422.
- [26] R. Perochon, F. Barrière, O. Jeannin, L. Piekara-Sady, M. Fourmigué, *Chem. Commun.* **2021**, 57, 1615–1618.
- [27] Z. W. Huang, V. Laurent, G. Chetouani, J. Y. Ljubimova, E. Holler, T. Benvegna, P. Loyer, S. Cammas-Marion, *Int. J. Pharm.* **2012**, 423, 84–92.
- [28] S. Cammas, I. Renard, V. Langlois, P. Guéri, *Polymer* **1996**, 37, 4215–4220.
- [29] D. K. Roper, W. Ahn, M. Hoepfner, *J. Phys. Chem. C* **2007**, 111, 3636–3641.
- [30] M. Ciancone, F. Camerel, *Chem. Commun.* **2017**, 53, 6339–6342.
- [31] M. Ciancone, N. Bellec, F. Camerel, *ChemPhotoChem* **2020**, 4, 5341–5345.
- [32] Z. Jiang, C. Zhang, X. Wang, M. Yan, Z. Ling, Y. Chen, Z. Liu, *Angew. Chem.* **2021**, 133, 22550–22558.
- [33] K. Chen, W. Fang, Q. Zhang, X. Jiang, Y. Chen, W. Xu, Q. Shen, P. Sun, W. Huang, *ACS Appl. Bio Mater.* **2021**, DOI 10.1021/acsbm.1c00168.

- [34] M. Han, B. Kim, H. Lim, H. Jang, E. Kim, *Adv. Mater.* **2020**, *32*, 1905096.
- [35] S. Li, Q. Deng, Y. Zhang, X. Li, G. Wen, X. Cui, Y. Wan, Y. Huang, J. Chen, Z. Liu, L. Wang, C.-S. Lee, *Adv. Mater.* **2020**, *32*, 2001146.
- [36] W. Jia, F. Huang, Q. Zhang, L. Zhao, C. Li, Y. Lu, *Chem. Commun.* **2022**, *58*, 6340–6343.
- [37] J. Li, L. Zheng, C. Li, Y. Xiao, J. Liu, S. Wu, B. Zhang, *Biomater. Sci.* **2021**, *9*, 4648–4661.
- [38] B. Li, H. Liu, Y. He, M. Zhao, C. Ge, M. R. Younis, P. Huang, X. Chen, J. Lin, *Angew. Chem. Int. Ed.* **2022**, *61*, e202200025.
- [39] H. Pan, S. Li, J. Kan, L. Gong, C. Lin, W. Liu, D. Qi, K. Wang, X. Yan, J. Jiang, *Chem. Sci.* **2019**, *10*, 8246–8252.
- [40] Y. Wang, K. Ogasahara, D. Tomihama, R. Mysliborski, M. Ishida, Y. Hong, Y. Notsuka, Y. Yamaoka, T. Murayama, A. Muranaka, M. Uchiyama, S. Mori, Y. Yasutake, S. Fukatsu, D. Kim, H. Furuta, *Angew. Chem.* **2020**, *132*, 16295–16300.
- [41] H. Casajus, E. Dubreucq, S. Tranchimand, V. Perrier, C. Nugier-Chauvin, S. Cammas-Marion, *Biomacromolecules* **2020**, *21*, 2874–2883.
- [42] O. Thioune, H. Fessi, J. P. Devissaguet, F. Puisieux, *Int. J. Pharm.* **1997**, *146*, 233–238.
- [43] M. G. Vargas Guerrero, J.-B. Pluta, N. Bellec, S. Cammas-Marion, F. Camerel, *Molecules* **2021**, *26*, 7703.
- [44] J.J. Wenz, *BBA - Biomembranes* **2018**, *1860*, 673–682.
- [45] A. A. Bunaciu, V. D. Hoang, H. Y. Aaboul-Enein, *Critical Reviews in Analytical Chemistry* **2015**, *45*, 156–165.

Entry for the Table of Contents

The photothermal properties of a series of hydrophobic gold-bis(dithiolene) absorbing in the NIR-III region were evaluated in organic solvents and in aqueous solution after encapsulation in polymer nanoparticles.

Institutional and author Twitter handles: @UnivRennes1 @chimie_ISCR @INC_CNRS @CammamMarion @RGuechaichia